# Comparative Performance of Multi-Platform DEMs and Topographic Sheets in Fluvial Morphometry: Insights from the Jiadhal River Basin, India

Ishanjyoti Chetia[1], and Bhagawat Pran Duarah[1*]
[1]Department of Geological Sciences, Gauhati University
[*]Corresponding author email: bpduarah@gmail.com

(Received on 4 March 2025; In final form on 14 August 2025)

***DOI:*** *https://doi.org/10.58825/jog.2025.19.2.236*

**Abstract**: This study evaluates the performance of various Digital Elevation Models (DEMs) and Survey of India (SOI) topographic sheets in fluvial morphometry using the upper part of the Jiadhal River basin as a case study. The primary objective is to compare and assess the interchangeability of data derived from SRTM, ASTER, AW3D, TanDEM-X, Cartosat 30m DEMs, and SOI 1:50,000 scale topographic sheets. Key morphometric parameters such as stream order, stream length, drainage density, drainage texture, basin area, perimeter, and relief aspects were derived from each dataset and compared to determine the influence of spatial resolution on hydrological studies. Results indicate that DEMs such as AW3D, Cartosat capture finer landform features better and provide added precision in stream delineation, mostly in flat terrains, as compared to other data sources. Despite variations in satellite's spatial resolutions, parameters and sensor systems, the derived fluvial morphometric parameters and statistics from the DEMs and topographic sheets showed significant agreement overall. The study highlights that AW3D, Cartosat 30m DEM outperforms SRTM, ASTER and TanDEM-X in stream path delineation, and are recommended for future morphometric and river basin studies. This research highlights the significance of choosing appropriate DEMs based on their spatial resolutions as well as terrain characteristics of the river basin for improved morphometric and river basin analysis.

**Keywords:** Basin Morphometry; Digital Elevation Model; AW3D; ASTER; SRTM; Cartosat; TanDEM-X; Toposheet

## 1. Introduction

Digital Elevation Models (DEMs) are remotely acquired data products represented in the form of arrays of pixels. Each pixel center represents the elevation of the area it covers (Guth et al., 2021). DEMs serve as essential inputs in studies involving landform evolution, morphotectonics, hydrological modelling (Croneborg et al., 2020). The efficacy of DEMs across various disciplines depends on the quality of the dataset, for example, the spatial resolution and vertical accuracy. Several factors contribute to the quality of DEMs, including the acquisition mode and the sensors configuration (Gesch, 2012).
DEMs are now becoming essential tools in hydrological investigation in a river basin, enabling the determination of flow path, extraction of drainage networks, river basin boundary delineation, and for assessment of linear, aerial, and relief aspects of a basin. The above mentioned parameters directly influence hydrological characteristics such as water flow and runoff in a river basin.

Before the arrival of digital elevation data, river basin studies relied heavily on surveyed topographic maps (Horton, 1932; Horton, 1945; Langbein, 1947; Strahler, 1950; Strahler, 1952a; Strahler, 1952b; Miller, 1953; Strahler, 1954; Strahler, 1958; Strahler, 1964). The emergence of Remote Sensing (RS) and Geographic Information Systems (GIS) along with the progress of various DEMs, has made river basin modeling more efficient and less time-consuming.
Several DEMs are found extensively used for basin analysis, including: SRTM (Space Shuttle Topographic Mission), ASTER (Advanced Spaceborne Thermal Emission and Reflection). These DEMs perform better in data analysis for various hydrological studies (Ahmed et al., 2010; Pareta and Pareta, 2011; Bogale, 2021; Shekar and Mathew, 2022). With the progression in the domain of space technology, many new DEMs have been introduced such as AW3D (Alos World 3D) , Cartosat, TanDEM-X and many more. These satellite sensors differ in the sensing mechanism used, viz., SRTM operates in the microwave range and acquires data via a single-pass interferometric Synthetic Aperture Radar (SAR), TanDEM-X DEM operated within X band of microwave range, Cartosat, ASTER and AW3D operate within the optical range and acquire data through stereo pair optical sensors. Each method has its own advantages and disadvantages, depending on terrain conditions (Lakshmi and Yarrakula, 2019).

Attempts have been made in the past to evaluate the performance of different DEMs across diverse applications. Deo et al. (2016) compared the vertical accuracy of TanDEM-X and CartoDEM in four selected Indian terrains and derived to a conclusion that TanDEM-X performed somewhat better in flat to hilly areas, but CartoDEM was found superior in rugged Himalayan terrain due to reduced radar layover and shadowing effects, suggesting the two datasets may be complementary. Grohmann (2018) compared TanDEM-X, AW3D, SRTM, and ASTER DEMs in different geomorphological terrains in Brazil and came to the conclusion that TanDEM-X and AW3D performed better in terms of vertical accuracy and surface details. Nagaveni et al. (2019) evaluated TanDEM-X and SRTM DEM in runoff estimation and observed that both the DEMs have produced different key parameters such as stream length and watershed area. Pandya et al.

(2024) has compared the performance of DEMs such as SRTM, ASTER, AW3D, Cartosat in hydrological study of upper Mahi river basin and found that AW3D is trailed by the Cartosat as the reliable and accurate among the freely available DEMs.

The current study aims to conduct a comparative analysis of different DEM sources — SRTM, ASTER, AW3D, TanDEM-X, Cartosat 30m DEM's along with Survey of India (SOI) topographic sheets (1:50000 scale). The study performs comparison of river basin morphometric datasets extracted from each source to determine whether these data sources can be used interchangeably for basin studies. For this study, the upper part of the Jiadhal river basin, located in the hilly terrain of the outer Himalayan litho-sequence of Arunachal Pradesh, has been selected.

## 2. Geographical Setting of the Jiadhal River Basin

The Jiadhal River is a sub-tributary of the Subansiri River, originating in the Outer Himalayas in West Siang district of Arunachal Pradesh. The river's catchment area is located between latitudes 27˚45'N and 27˚34'N, and longitudes 94˚15'E and 94˚37'E. It has three tributaries: the Siri, the Sika, and the Sido (Figure 1). The Siri River originates in the northeastern part of the catchment and initially flows southward before turning westward. The Sika River begins in the northern part of the basin and flows south. The Sido River starts in the west and flows eastward.

These three rivers converge at a location known as *Trimukh* (mouth of three rivers) at the coordinate 27˚38'N, 94˚25.5'E. From this point onward, the river is named as Jiadhal. The river then flows southward and enters the plains of Assam near Jiadhalmukh in Dhemaji district. After continuing a few kilometers further, it joins the Subansiri River near Ghagarmukh.

The study area, located within the upper part of the Jiadhal River basin, is situated in the Himalayan terrain. The basin falls under a zone of subtropical monsoon climate (Das, 2013). The catchment area experiences minimal rainfall during November to February, with approximately 95% of precipitation occurring between March and October. The average annual rainfall in the region ranges from 2,965 mm to 4,386 mm, with a mean annual rainfall of about 3,150 mm (Das, 2013).

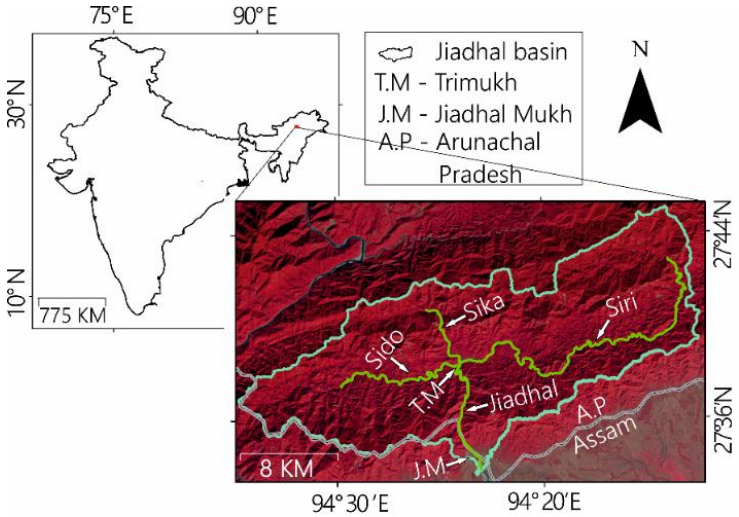


**Figure 1.** The river basin boundary, located within the Himalayan terrain, along with its three major tributaries—Sido, Sika, and Siri—are shown in the figure. The background of the figure is based on IRS LISS IV satellite imagery, which was acquired in January 2023.

## 3. Materials and Methods

### 3.1 Materials

The morphometric datasets were generated from six different sources

- SOI topographic sheet (no. 83I/6, 83I/10) of 1:50000 available in the Department of Geological Sciences, Gauhati University and also downloaded from https://www.surveyofindia.gov.in
- SRTM 30m DEM downloaded from https://earthexplorer.usgs.gov
- ASTER 30m DEM downloaded from https://search.earthdata.nasa.gov
- AW3D 30m DEM downloaded from https://portal.opentopography.org
- TanDEM-X 30m DEM downloaded from https://geoservice.dlr.de
- Cartosat 30m DEM downloaded from https://bhoonidhi.nrsc.gov.in/

### 3.2 Method

The downloaded topographic sheets were projected into Universal Transverse Mercator (UTM) zone 46N in QGIS version 3.36.3. From the merged topographic sheet, order wise streams were traced down starting with 1st order and

continuing to the highest order. This was done by creating a polyline shapefile. The boundary of the river basin was carefully traced by identifying the drainage divide from the map. A polygon shapefile (projection: UTM Zone 46N) was created to define the basin boundary. The boundary of the basin was then traced out from the map carefully by identifying the drainage divide by creating a polygon shapefile (projection: UTM zone 46N). Parameters such as stream number, stream length, area and perimeter were extracted automatically. Other morphometric parameters were derived using the mathematical formulae shown in Table 1.

All the DEMs except for the Cartosat perfectly cover the entire river basin and the morphometric parameter are extracted for the entire basin that lies within the hilly terrain. For the Cartosat DEM, there were some missing tiles within the river basin and this led to the extraction of parameters only for those parts of the basin where DEM titles were available. Thus, for the comparison of Cartosat datasets, the Sido River basin, which is a 6$^{th}$ order river basin of the river Jiadhal, was chosen and compared with optically derived AW3D DEM since AW3D extracted catchment parameter, viz., watershed boundary fits well with the topographic sheet delineated boundary.

The first step when working with a DEM is to address pixels, which are typically characterized by anomalous elevation values lower than the surrounding pixels (Krupavathi et al., 2024). These anomalous pixels, known as sinks, pits, or flats, arise due to the limited vertical accuracy and horizontal resolution of the DEM (Reuter et al., 2009). To resolve this problem, the elevation values of these pixels are adjusted by averaging eight neighboring pixels (Peckham, 2009). Following this, flow directions are assigned to each pixel based on maximum drop from the neighborhood pixels (Bhanudas et al., 2017). Using this information, the stream networks and basin boundaries are delineated.

For the derivation of morphometric parameters from the DEMs, the GIS-based software **Rivertools version 3.0** was used. Rivertools is a user-friendly software toolkit designed specifically for working with DEMs to extract hydrological geomorphological parameter (Peckham, 2009).

**Table 1.** Morphometric parameters used in the study.

| | Morphometric Parameters | Symbols | Formulas | Units | References |
|---|---|---|---|---|---|
| | | | **Linear Aspect** | | |
| **1.** | Number of streams within a given order | $N_u$ | | N/A | Horton R.E, 1945 |
| **2.** | Stream order | U | Hierarchical rank | N/A | Strahler A.N, 1957 |
| **3.** | Mean bifurcation ratio | η | $\eta = \sum R_b/n$<br>n=number of observations<br>$R_b$ = Bifurcation ratio. | Dimensionless | Horton R.E, 1945 |
| | | | **Areal Parameter** | | |
| **1.** | Area of the basin | A | | $Km^2$ | |
| **2.** | Perimeter of the basin | P | | Km | |
| **3.** | Drainage density | $D_d$ | $D_d = \sum L_u/A$<br>$\sum L_u$= Sum of length of streams of all order | $Km^{-1}$ | Horton R.E, 1945 |
| **4.** | Stream frequency | $F_s$ | $F_s = \sum N_u/A$<br>$\sum N_U$= Total number of streams of all order.<br>A= Total area of the basin | $Km^{-2}$ | Horton R.E, 1932 |
| **5.** | Drainage texture | $D_t$ | $D_t = \sum N_u/P$<br>P= Perimeter of the basin | $Km^{-1}$ | Horton R.E, 1945 |
| **6.** | Circularity ratio | $C_r$ | $A / A_p$<br>$A_p$= Area of the circle of same basin perimeter, | Dimensionless | Miller V.C, 1953 |
| | | | **Relief Parameter** | | |
| **1.** | Hypsometric integral | HI | HI = (mean elevation – minimum elevation)/ (maximum elevation - minimum elevation) | Dimensionless | Strahler A.N, 1952b |
| **2.** | | | Longitudinal profile | | |

## 4. Results and Discussion

To test the interchangeability of data sources in river basin morphometric analysis, several important parameters related to the linear, aerial, and relief aspects were selected for comparison.

### 4.1 Linear aspects

For the linear aspect, the parameters considered for comparisons are - stream numbers, stream order and bifurcation ratio.

#### 4.1.1 Stream numbers and Bifurcation ratio

The stream network derived from the topographic sheet indicates that the highest stream order is 6th, while all the 30m DEMs (SRTM, ASTER, AW3D, TanDEM-X, Cartosat) show the highest order as 7th. This discrepancy arises due to differences in the spatial resolution between the data sources. Finer resolution data products, such as the 30m DEMs, allow users to detect slightest elevation variations and small landform features more accurately than coarser resolution counterpart (Niyazi et al., 2019; Roy et al., 2025). As a result, finer resolution data detects more detailed streams, leading to a higher stream count compared to coarser resolution data.

The stream counts from all sources are shown in Table 2. Stream count for Sido basin from AW3D and Cartosat is shown in Table 3. Despite the differences in stream count, the mean bifurcation ratio (Bf) calculated from each data source is quite similar. Specifically, topographic sheet-derived mean Bf: 4.25, AW3D-derived mean Bf: 4.26, SRTM-derived mean Bf: 4.33, ASTER-derived mean Bf: 4.4, TanDEM-X-derived mean Bf: 4.33, Cartosat-derived mean Bf: 4.03. The stream networks derived from these six sources are shown in Figure 2. For the Sido River, AW3D derived mean Bf: 4.64, and Cartosat derived mean Bf: 4.46.

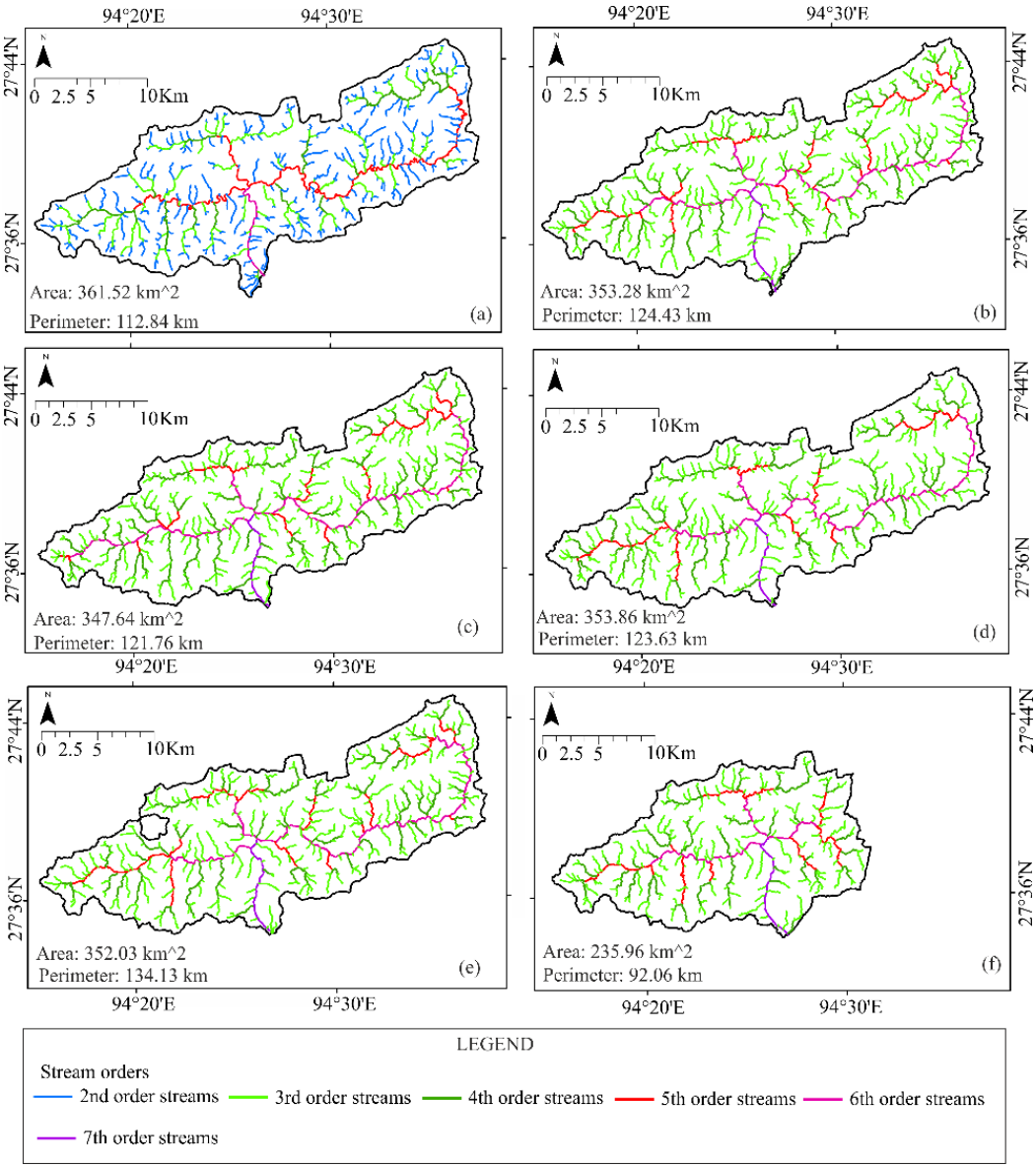


**Figure 2**. Basin boundary and stream network extracted from topographic sheet (a), SRTM (b), ASTER (c), AW3D (d), TanDEM-X (e), and Cartosat (f). For better visualization, the 1st order streams have been excluded from the topographic sheet, and both the 1st and 2nd order streams have been omitted from the DEMs.

**Table 2**. Order wise stream count derived from all the data sources are shown in the table.

| | Topographic sheet | AW3d | SRTM | ASTER | TanDEM-X | Cartosat |
|---|---|---|---|---|---|---|
| 1st order | 1268 | 5418 | 6243 | 6574 | 6092 | 3968 |
| 2nd order | 303 | 1140 | 1279 | 1377 | 1295 | 851 |
| 3rd order | 69 | 250 | 283 | 321 | 283 | 186 |
| 4th order | 17 | 57 | 66 | 70 | 64 | 44 |
| 5th order | 3 | 11 | 17 | 16 | 15 | 10 |
| 6th order | 1 | 3 | 3 | 3 | 3 | 3 |
| 7th order | | 1 | 1 | 1 | 1 | 1 |
| Total | 1661 | 6880 | 7892 | 8362 | 7753 | 5023 |

**Table 3.** Order wise stream count for Sido River basin as compared from AW3D and Cartosat.

| | 1st | 2nd | 3rd | 4th | 5th | 6th |
|---|---|---|---|---|---|---|
| AW3D | 1830 | 382 | 81 | 20 | 3 | 1 |
| Cartosat | 1730 | 366 | 81 | 21 | 5 | 1 |

**4.1.2 Stream Length**

The presence of anomalous pixel value due to vertical or horizontal resolutions significantly influences the stream path and length (Rana and Suryanarayana, 2019) and to avoid them these anomalous pixels are replaced by neighbourhood pixel averaging as mentioned in the methodology. The more such pixels present in a DEM, the greater the deviation of the stream path from the actual flow path. The total stream length measured for each order is shown in Table 4**.**

For a detailed comparison of stream length, the basin lengths of the Sido, Sika, and Siri River basins were selected. The measured results are presented in Table 5.
The measurements derived from the DEMs show considerable variation compared to the topographic sheet. The Siri River basin shows the highest variation, followed by the Sido River basin, and the least variation is observed in the Sika River basin. The area through which the Siri River flows is a flat, depressed zone (Figure 3), where the DEMs were unable to accurately delineate the flow path (Garbrecht and Martz, 1997). This deviation results in a shorter stream length compared to the topographic sheet. On the other hand, the Siri River flows through a relatively steeper area, where the stream length does not vary much. The Sido River flows through a moderately steep area, showing a moderate deviation in basin length compared to the Siri River.

Despite the variations in flow path and length, the AW3D dataset provides the most accurate flow path delineation when compared to the other three DEMs (ASTER, SRTM, TanDEM-X) as evidenced in Figure 4. Cartosat derived stream network of Sido basin is compared with AW3D derived stream network shown in Figure 5. Cartosat derived stream network shows similar flow path to AW3D derived stream network.

**Table 4**. Showing total stream length per stream order in km measured from each data source.

| | Topographic sheet | AW3d | SRTM | ASTER | TanDEM-X |
|---|---|---|---|---|---|
| 1st order | 669.62 | 838.93 | 977.71 | 965.92 | 953.90 |
| 2nd order | 212.40 | 412.96 | 414.12 | 430.35 | 435.00 |
| 3rd order | 103.11 | 214.16 | 231.64 | 226.88 | 240.00 |
| 4th order | 45.18 | 104.20 | 100.64 | 125.18 | 111.84 |
| 5th order | 57.83 | 38.61 | 51.41 | 40.49 | 49.70 |
| 6th order | 10.57 | 46.04 | 47.05 | 53.66 | 47.23 |
| 7th order | | 9.09 | 9.25 | 9.38 | 10.05 |
| Total | 1098.71 | 1663.99 | 1831.82 | 1851.86 | 1847.72 |

**Table 5.** Longest channel length measured from each of the data source in km.

| Data sources | Sido River | Sika River | Siri River |
|---|---|---|---|
| Topographic sheet | 24.33 | 14.00 | 50.62 |
| AW3d | 22.60 | 14.70 | 45.42 |
| SRTM | 21.60 | 14.72 | 43.34 |
| ASTER | 21.80 | 15.11 | 42.33 |
| TanDEM-X | 22.15 | 15.86 | 43.37 |
| Cartosat | 21.01 | _- | - |

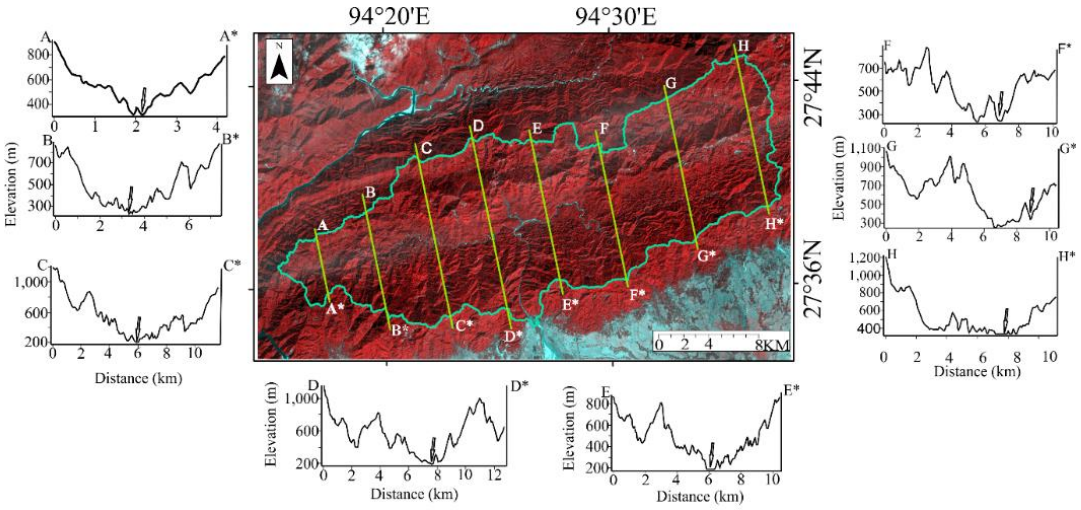


**Figure 3.** Cross profiles of the river basin, showing that the middle portion through which the Siri and Sido rivers flow is a flat, depressed zone. The cross profiles were prepared using the AW3D 30m DEM**,** with the background provided **by** IRS LISS IV satellite imagery**,** acquired in January 2023. The arrows on the cross profiles indicate the positions of the rivers.

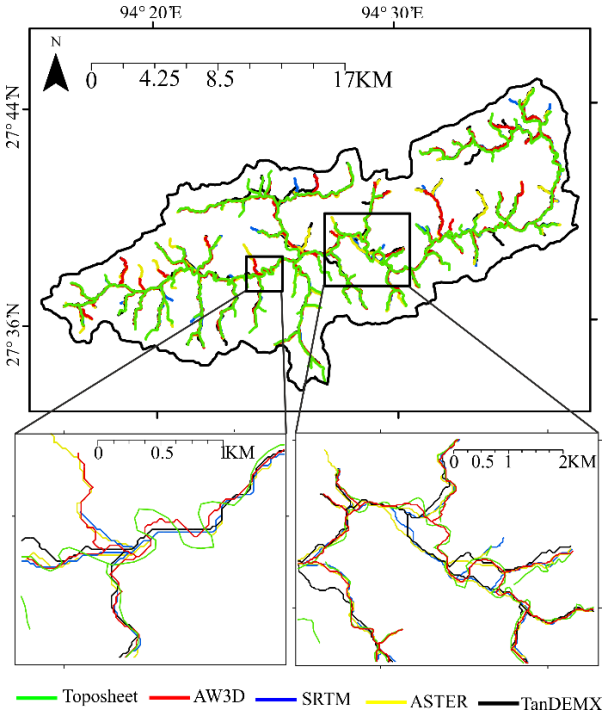


**Figure 4.** Comparison of stream networks delineated from all the data sources. The zoomed-in portion highlights the deviation of the stream path from the actual flow path. Different colours are used to demarcate the various data sources.

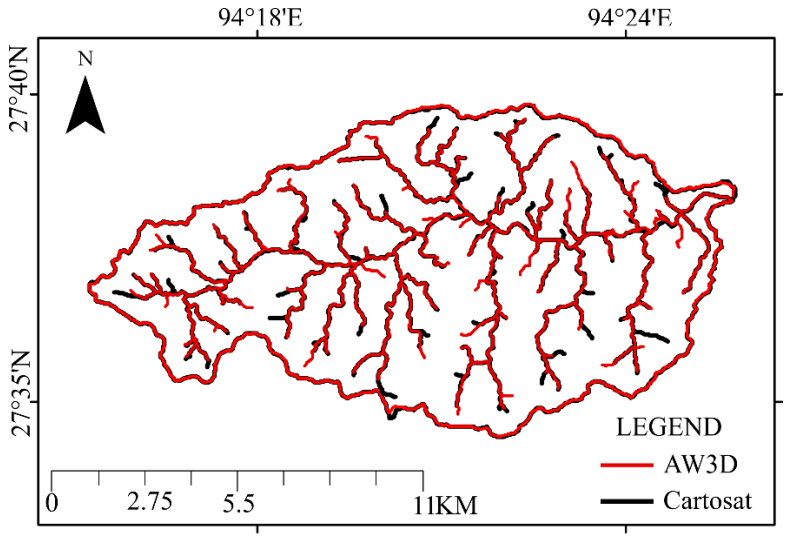


**Figure 5.** Stream network derived from Cartosat and AW3D is shown for the Sido basin. The comparison reveals that both AW3d and Cartosat derived stream network shows similar flow paths.

### 4.2 Aerial aspects

Under aerial aspect, parameters such as area, perimeter of the basin, drainage density, stream frequency, drainage texture, circularity ratio are considered.

#### 4.2.1 Area and perimeter

The area and perimeter of a river basin are key parameters that determine the volume of runoff generated within the basin (Desta et al., 2005). These parameters also contribute to the derivation of other important morphometric parameters. The basin area delineated from each data source showed similar results, i.e., 361.52 $km^2$ (topographic sheet), 353.28 $km^2$ (SRTM), 353.86 $km^2$ (AW3D), 347.64 $km^2$ (ASTER), 352.03 $km^2$ (TanDEM-X). But all the DEM derived perimeter values are higher than topographic sheet 112.84 km (Topographic sheet), 124.43 km (SRTM), 123.63 km (AW3D), 121.76 km (ASTER), and 134 km (TanDEM-X).

Cartosat derived basin area and perimeter of the Sido River basin are calculated as 108.38 sq. km and 55.87 km while AW3D derived basin area and perimeter for the same basin is calculated as 108.48 sq. km and 55.30 km.

#### 4.2.2 Drainage density, stream frequency, drainage texture

The derivation of drainage density, stream frequency, and drainage texture depends on total stream counts, total stream length, basin area, and basin perimeter (Horton R.E, 1932; Horton R.E, 1945). There was a significant difference in the stream count and stream length between the topographic sheet and the DEMs due to differences in spatial resolutions which, in turn, influence the derived parameters.

The derivations of drainage density, stream frequency, drainage texture depends on total stream counts, total stream length, basin area and basin perimeter (Horton R.E, 1932; Horton R.E, 1945). The total stream counts and stream length derived from topographic sheet shows vast differences when compared to the DEMs resulting from difference in spatial resolutions. Topographic sheet derived drainage density is measured as 3.04, while SRTM measures 5.18, ASTER measures 5.33, AW3d measures 4.70 and TanDEM-X measures 5.24. Stream frequency are measured as 4.59, 22.33, 24.05, 19.44, and 22.02 from topographic sheet, SRTM, ASTER and AW3D, TanDEM-X DEMs respectively. Drainage textures are measured as 14.72, 63.42, 68.67, 55.64, 57.85 from topographic sheet, SRTM, ASTER, AW3D, TanDEM-X DEMs respectively. Cartosat derived values of drainage density, stream frequency, drainage texture for the Sido River basin are calculated as 4.61, 20.87, 40.49, while AW3D derived values of drainage density, stream frequency, drainage texture for the same basin are calculated as 4.62, 21.36, 41.89 respectively.

#### 4.2.3 Circularity ratio

The circularity ratio is a parameter that depends on the basin area and perimeter (Miller, 1953). Since the parameter did not vary significantly between the topographic sheet and the DEMs, the results for all datasets were similar. However, TanDEM-X shows maximum variation from the toposheet derived value.

Topographic sheet derived circularity ratio is measured as 0.36. The SRTM derived circularity ratio is measured as 0.29, AW3D derived value is 0.29, ASTER derived value is 0.30, TanDEM-X derived values is 0.25.

Cartosat derived circularity ratio for the Sido River basin is measured as 0.43 and AW3D derived value is measured as 0.44.

### 4.3 Relief Aspects

Hypsometry is the distribution of land surface area with respect to height (Miller, 1953). The concept was introduced by Langbein in year 1947 (Langbein 1947). Strahler extended this concept by introducing the percentage hypsometric curve (PHC) and hypsometric integral (HI) values (Strahler, 1952b). Key relief parameters, such as the percentage hypsometric curve (PHC) and hypsometric integral (HI) values, extracted from all the DEMs show a similar concave-upward profile,

as shown in Figure 6a and Figure 7a. The HI values are comparable across all the datasets.

The longitudinal profile of a river is defined as the gradient of the water surface line from the river source to its mouth. This profile can be constructed by plotting elevation data against distance from the source along the river's course. The comparison of longitudinal profiles derived from all the DEMs shows contrasting results. This variation can be attributed to the differences in the flow path of the streams or the vertical accuracy of the DEMs, as shown in Figure 6b and Figure 7b.

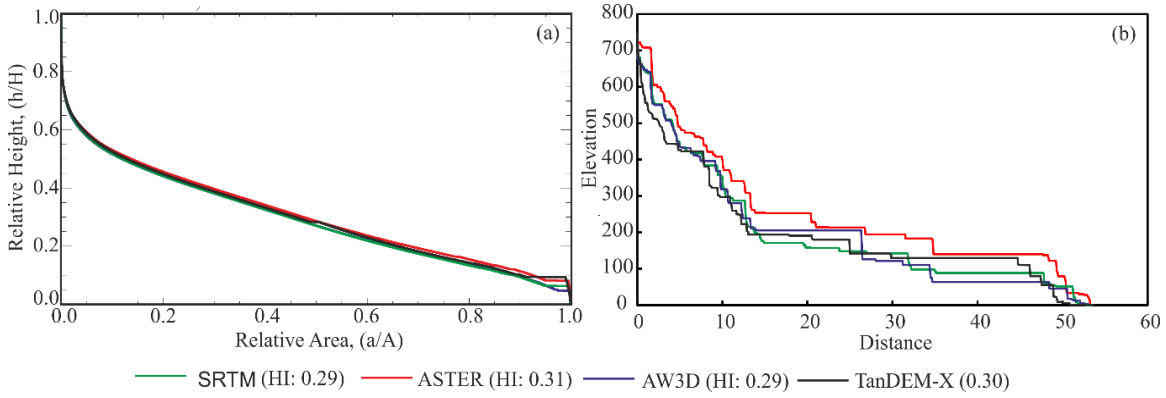


**Figure 6a.** Percentage hypsometric curve and (b) longitudinal profile for the river basin, derived from SRTM, ASTER, AW3D DEMs, TanDEM-X. The hypsometric integral (HI) values are indicated. Colour lines are used to indicate the different data sources.

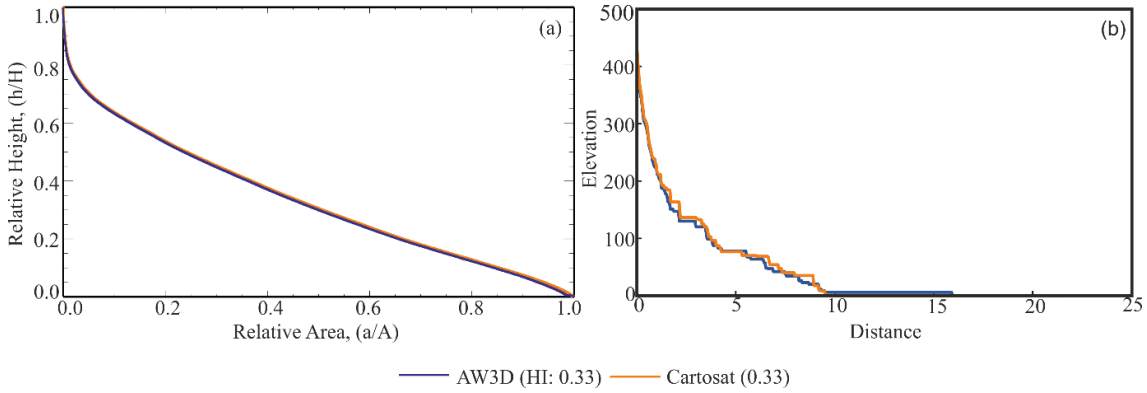


**Figure 7a.** Percentage hypsometric curve and (b) longitudinal profile for the Sido River basin, derived from AW3D and Cartosat DEM. The hypsometric integral (HI) values are indicated. Colour lines are used to indicate the different data sources.

## 5. Conclusions

A comparative analysis of morphometric parameters derived from SOI 1:50,000 scale topographic sheets**,** SRTM**,** ASTER**,** AW3D, TanDEM-X, Cartosat 30m DEMs was conducted to test the interchangeability and reliability of these datasets. The study focused on the upper catchment of the Jiadhal River basin**,** located in the hilly terrain of the Himalayas.

For the entire hilly part of the basin, some of the tiles of Cartosat were missing, which has set limitation to extract morphometric parameter for the entire basin. Thus only

Sido River ($6^{th}$ order sub-basin) was chosen for comparison for Cartosat data. The comparison is also done with the data sets derived from AW3D for the same basin. The results indicate that both vertical and horizontal resolutions significantly influence morphometric parameters. Finer resolution data sources, such as the 30m DEMs, have a greater ability to detect minor landform features, as evidenced by differences in stream order and stream numbers generated from the various data sources. Accurate delineation of stream paths and lengths depends on the presence of anomalous pixels (voids). These voids can cause deviations in the stream path, leading to errors in stream length. Among the datasets, AW3D 30m DEM outperforms SRTM**,** ASTER and TanDEM-X in accurately delineating stream paths, especially in flat zones. While comparison of Cartosat derived stream network for the Sido sub-basin with AW3D DEM shows similar result and both the DEMs performs well in stream path delineation.

Furthermore, the volume of runoff generated from rainfall events is influenced by the size of the river basin. Therefore, the area and perimeter of the basin are crucial parameters. The values extracted for these parameters from all data sources show approximately similar results. However, the shape of the drainage basin extracted from TanDEM-X shows substantial deviation from all the other

DEMs and can be evidenced from the value of circularity ratio which is significantly different from the other DEMs and the toposheet. Comparison of Cartosat derived Sido River basin with AW3d show similar boundary and the circularity ratio yield similar values.

In conclusion, differences in spatial resolutions have resulted variations in the morphometric parameter values between the topographic sheet and the DEMs. However, the values extracted from the DEMs show strong agreement among them overall. In certain cases, AW3D 30m DEM outperforms SRTM**,** ASTER**,** TanDEM-X especially in terms of stream path delineation. Moreover, comparison of Cartosat derived dataset with AW3D DEM shows that both the DEMs performs better than the rest of the DEMs. Therefore, both, the AW3D 30m DEM and Cartosat DEM are recommended for studies involving river basin modeling due to their superior accuracy in stream path delineation compared to the other two datasets. In case, if Cartosat DEM tiles are not fully available for any study region, then Alos World 3D can be used interchangeability.

## Declarations

**Acknowledgement**
The authors are thankful to the websites https://earthexplorer.usgs.gov, https://search.earthdata.nasa.gov, https://bhukosh.gsi.gov.in, https://crudata.uea.ac.uk/cru/data/ hng, https://portal.opentopography.org, https://geoservice. dlr.de, https://bhoonidhi.nrsc. gov.in/ for giving us the opportunity to the access their open source data products. They are thankful to the Head of the Department of Geological Sciences, Gauhati University, Assam, India for providing research facilities. They are also thankful to the anonymous reviewers for their valuable suggestion which has helped the authors to improve the quality of the manuscript.

**Funding**
No funding was received to assist with the preparation of this manuscript.

**Conflict of Interest**
The authors declare no conflict of interests.

**Data Availability**
The data that support the findings of this study are available on request from the corresponding author, B. P. Duarah.

**Code Availability**
Not Applicable.

**Author contributions**
Both the authors contributed to the study. Bhagawat Pran Duarah conceptualized and designed the work. Material preparation, data collection and analysis were performed by Ishanjyoti Chetia. The final draft of the manuscript was written by Ishanjyoti Chetia. Final review of the manuscript was performed by Bhagawat Pran Duarah. Both the authors read and approved the final manuscript.

## References

Ahmed, S. A., K. N. Chandrashekarappa, S. K. Raj, V. Nischitha and G. Kavitha (2010). Evaluation of morphometric parameters derived from ASTER and SRTM DEM—A study on Bandihole sub-watershed basin in Karnataka. Journal of the Indian Society of Remote Sensing, 38(2), pp. 227–238. https://doi.org/10.1007/s12524-010-0029

Bhanudas, K. T., K. Balasubramani and M. Gomathi (2017). Comparative analysis of CARTOSAT, ASTER and SRTM digital elevation models of different terrains for extraction of watershed parameters. Available at: https://www.researchgate.net/publication/321272177

Bogale, A. (2021). Morphometric analysis of a drainage basin using geographical information system in Gilgel Abay watershed, Lake Tana Basin, upper Blue Nile Basin, Ethiopia. Applied Water Science, 11(7), 122. https://doi.org/10.1007/s13201-021-01447-9

Croneborg, L., K. Saito, M. Matera, D. McKeown and J. Van Aardt (2020). Digital elevation models: A guidance note on how digital elevation models are created and used – includes key definitions, sample terms of reference, and how best to plan a DEM mission. World Bank Group, Washington, D.C. Available at: http://documents.worldbank.org/cirated/en/667961599807477538

Das, P. J. (2013). Jadhal River Catchment, Assam, India: Building community capacity for flash flood risk management. Case Studies on Flash Flood Risk Management in the Himalayas, In Support of Specific Flash Flood Policies. Available at: http://lib.icimod.org/record/27767

Deo, R., M. Jain and Y. S. Rao (2016). Comparison of TanDEM-X and Cartosat-1 stereo DEMs over different terrains of India. 2016 IEEE International Geoscience and Remote Sensing Symposium (IGARSS), 10–15 July 2016. doi:10.1109/IGARSS.2016.7730694

Desta, L., V. Carucci, A. Wendem-Agenehu and Y. Abebe (2005). Community based participatory watershed development: A guideline, 1st edn. Ministry of Agriculture and Rural Development (MoARD), Addis Ababa, Ethiopia.

Garbrecht, J. and L. W. Martz (1997). The assignment of drainage direction over flat surfaces in raster digital elevation models. Journal of Hydrology, 193, pp. 204–213.

Gesch, D. B. (2012). Global digital elevation model development from satellite remote sensing data. In Yang, X. and Li, J. (eds.) Advances in Mapping from Remote Sensor Imagery: Techniques and Applications. pp. 92–109.

Grohmann, C. H. (2018). Evaluation of TanDEM-X DEMs on selected Brazilian sites: comparison with SRTM, ASTER GDEM and ALOS AW3D30. Remote

Sensing of Environment, 212, pp. 121–133. https://doi.org/10.1016/j.rse.2018.04.043

Guth, P. L., A. Van Niekerk, C. H. Grohmann, J.-P. Muller, L. Hawker, I. V. Florinsky, D. Gesch, H. I. Reuter, V. Herrera-Cruz, S. Riazanoff, C. López-Vázquez, C. C. Carabajal, C. Albinet and P. Strobl (2021). Digital elevation models: Terminology and definitions. Remote Sensing, 13(18), 3581. https://doi.org/10.3390/rs13183581

Horton, R. E. (1932). Drainage-basin characteristics. Transactions of the American Geophysical Union, 13(1), pp. 350–361. https://doi.org/10.1029/TR013i001p00350

Horton, R. E. (1945). Erosional development of streams and their drainage basins: hydrophysical approach to quantitative morphology. Geological Society of America Bulletin, 56(3), pp. 275–370.

Krupavathi, C., S. S. Gowd, M. Rajasekhar and P. Ravikumar (2024). Morphometric analysis of Mogamureru river basin at the YSR Kadapa District, Andhra Pradesh, India using GIS and remote sensing. Geomatica, 76(1), 100005. https://doi.org/10.1016/j.geomat.2024.100005

Lakshmi, S. E. and K. Yarrakula (2019). Review and critical analysis on digital elevation models. Geofizika, 35(2), pp. 129–157. https://doi.org/10.15233/gfz.2018.35.7

Langbein, W. B. (1947). Topographic characteristics of drainage basins. U.S. Geological Survey Water-Supply Paper, 968, pp. 125–157.

Miller, V. C. (1953). A quantitative geomorphic study of drainage basin characteristics in the Clinch Mountain area, Virginia and Tennessee. Technical Report, No. 3, Columbia University Department of Geology.

Nagaveni, C., K. P. Kumar and M. V. Ravibabu (2019). Evaluation of TanDEM-X and SRTM DEM on watershed simulated runoff estimation. Journal of Earth System Science, 128(2). https://doi.org/10.1007/s12040-018-1035-z

Niyazi, B., S. Zaidi and M. Masoud (2019). Comparative study of different types of digital elevation models on the basis of drainage morphometric parameters (Case study of Wadi Fatimah Basin, KSA). Earth Systems and Environment, 3(3), pp. 539–550. https://doi.org/10.1007/s41748-019-00111-2

Pandya, D., V. K. Rana and T. M. V. Suryanarayana (2024). Inter-comparison and assessment of digital elevation models for hydrological applications in the Upper Mahi River Basin. Applied Geomatics, 16(1), pp. 191–214. https://doi.org/10.1007/s12518-023-00547-2

Pareta, K. and U. Pareta (2011). Quantitative morphometric analysis of a watershed of Yamuna basin, India using ASTER (DEM) data and GIS. International Journal of Geomatics and Geosciences, 2(1), pp. 248–269.

Peckham, S. D. (2009). Geomorphometry in RiverTools. in Hengl, T. and H. I. Reuter (eds.) Geomorphometry: Concepts, software, applications. Developments in Soil Science, Vol. 33. Elsevier, pp. 411–430. https://doi.org/10.1016/S0166-2481(08)00018-4

Rana, V. K. and T. M. V. Suryanarayana (2019). Visual and statistical comparison of ASTER, SRTM, and Cartosat digital elevation models for watershed. Journal of Geovisualization and Spatial Analysis, 3(2). https://doi.org/10.1007/s41651-019-0036-z

Reuter, H. I., T. Hengl, P. Gessler and P. Soille (2009). Preparation of DEMs for geomorphometric analysis. In Hengl, T. and H. I. Reuter (eds.) Geomorphometry: Concepts, software, applications. Developments in Soil Science, Vol. 33. Elsevier, pp. 87–120. https://doi.org/10.1016/S0166-2481(08)00004-4

Roy, S., M. G. Uddin, K. Abdelrahman, M. S. Fnais and M. Abioui (2025). Assessing the impact of digital elevation model resolution on hypsometric analysis in large river basins (India): A non-parametric statistical approach. Earth Science Informatics, 18(1). https://doi.org/10.1007/s12145-024-01607-w

Shekar, P. R. and A. Mathew (2022). Morphometric analysis for prioritizing sub-watersheds of Murredu River basin, Telangana State, India, using a geographical information system. The Journal of Engineering and Applied Science, 69(1), p. 44. https://doi.org/10.1186/s44147-022-00094-4

Strahler, A. N. (1950). Davis' concepts of slope development viewed in the light of recent quantitative investigations. Annals of the Association of American Geographers, 40(3), pp. 209–213.

Strahler, A. N. (1952a). Dynamic basis of geomorphology. Geological Society of America Bulletin, 63(9), pp. 923–938. https://doi.org/10.1130/0016-7606(1952)63[923:DBOG]2.0.CO;2

Strahler, A. N. (1952b). Hypsometric (area-altitude) analysis of erosional topography. Geological Society of America Bulletin, 63(11), pp. 1117–1142.

Strahler, A. N. (1954). Statistical analysis in geomorphic research. Journal of Geology, 62(1), pp. 1–25.

Strahler, A. N. (1957). Quantitative analysis of watershed geomorphology. Transactions of the American Geophysical Union, 38(6), pp. 913–920. https://doi.org/10.1029/TR038i006p00913

Strahler, A. N. (1958). Dimensional analysis applied to fluvially eroded landforms. Geological Society of America Bulletin, 69(3), pp. 279–300.

Strahler, A. N. (1964). Quantitative geomorphology of drainage basins and channel networks. In Chow, V. T. (ed.) Handbook of Applied Hydrology. McGraw-Hill, New York, pp. 4-39–4-76.